Fis1p and Caf4p, but not Mdv1p, determine the polar localization of Dnm1p clusters on the mitochondrial surface

Astrid C. Schauss, Jörg Bewersdorf* and Stefan Jakobs‡

Max-Planck Institute for Biophysical Chemistry, Department of NanoBiophotonics, Am Fassberg 11, 37077 Göttingen, Germany
*Present address: Institute for Molecular Biophysics, The Jackson Laboratory, 600 Main Street, Bar Harbor, ME 04609, USA
‡Author for correspondence (e-mail: sjakobs@gwdg.de)

Accepted 27 April 2006
Journal of Cell Science 119, 3098-3106 Published by The Company of Biologists 2006
doi:10.1242/jcs.03026

Summary

The mitochondrial division machinery consists of the large dynamin-related protein Dnm1p (Drp1/Dlp1 in humans), and Fis1p, Mdv1p and Caf4p. Proper assembly of Dnm1p complexes on the mitochondrial surface is crucial for balanced fission and fusion events. Using quantitative confocal microscopy, we show that Caf4p is important for the recruitment of Dnm1p to the mitochondria. The mitochondrial Dnm1p assemblies can be divided into at least two morphologically distinguishable fractions. A small subset of these assemblies appear to be present as Dnm1p-spirals (or rings) that encircle tubule constrictions, with seldom more than seven turns. A larger fraction of the Dnm1p assemblies is primarily present at one side of the mitochondrial tubules. We show that a majority of these mitochondria-associated Dnm1p clusters point towards the cell cortex. This polarized orientation is abolished in *fis1Δ* and *caf4Δ* yeast cells, but is maintained in *mdv1Δ* cells and after disruption of the actin cytoskeleton. This study suggests that Caf4p plays a key role in determining the polarized localization of those Dnm1p clusters that are not immediately involved in the mitochondrial fission process.

Supplementary material available online at
http://jcs.biologists.org/cgi/content/full/119/15/3098/DC1

Key words: Actin, Dnm1, Dynamin, Fluorescence microscopy, Mitochondrial fission, Polarity

Introduction

Mitochondria are ubiquitous and essential organelles of eukaryotic cells. In many cell types, ranging from yeast to man, the mitochondria form dynamic networks that undergo continuous fission and fusion (Bereiter-Hahn and Voth, 1994; Nunnari et al., 1997). Besides being essential for mitochondrial shape, recent studies have highlighted the role of the mitochondrial fission machinery in the regulation of programmed cell death (Fannjiang et al., 2004; Frank et al., 2001; Jagasia et al., 2005; Youle and Karbowski, 2005).

A key component of the mitochondrial fission machinery is a dynamin-related large GTPase, termed Dnm1p in the budding yeast *Saccharomyces cerevisiae* or Drp1 in mammals (Bleazard et al., 1999; Otsuga et al., 1998; Sesaki and Jensen, 1999; Smirnova et al., 1998). Dnm1/Drp1 form assemblies that are primarily associated to the mitochondrial surface, occasionally at points of tubule constriction and fission (Bleazard et al., 1999; Legesse-Miller et al., 2003; Otsuga et al., 1998; Sesaki and Jensen, 1999). At such constrictions the membranes are squeezed together but the mitochondria are luminal contiguous (Jakobs et al., 2003b). Based on biochemical and structural analysis of purified Dnm1p, it has been suggested that Dnm1p/Drp1 assemblies form spiral-like structures around constricted mitochondrial tubules to drive mitochondrial division (Ingerman et al., 2005). Although the precise mechanism remains controversial, GTP hydrolysis might induce a conformational change of spiral-like Dnm1p-structures resulting in tubule scission at these constricted sites. In *S. cerevisiae*, genetic, cytological and biochemical data demonstrate that Dnm1p acts in concert with Mdv1p and Fis1p to mediate fission (for reviews, see Jensen, 2005; Okamoto and Shaw, 2005; Scott et al., 2003; Shaw and Nunnari, 2002; Yaffe, 1999). In addition, Caf4p has recently been identified as a new component of the fission machinery (Griffin et al., 2005). Caf4p interacts with Dnm1p, Mdv1p and Fis1p. It is the nearest homologue of Mdv1p in *S. cerevisiae*. Both are WD40 proteins of approximately 80 kDa with an N-terminal extension, a central coiled-coil domain and a C-terminal WD40 repeat domain (Cerveny et al., 2001; Fekkes et al., 2000; Tieu and Nunnari, 2000). Fis1p is a small (18 kDa) integral protein of the outer membrane, with its C-terminus exposed to the intermembrane space and its N-terminus facing the cytoplasm (Mozdy et al., 2000; Tieu and Nunnari, 2000). It is uniformly distributed along mitochondrial tubules (Mozdy et al., 2000) and has at least two independent functions in the fission pathway (Tieu et al., 2002). Early in the fission pathway, Fis1p targets Dnm1p to mitochondrial membranes through Mdv1p or Caf4p, which both act as molecular adaptors (Griffin et al., 2005). Later, at a rate-limiting step, Fis1p acts together with Dnm1p and Mdv1p in the actual fission process (Cerveny and Jensen, 2003; Shaw and Nunnari, 2002; Tieu et al., 2002). Unlike Mdv1p and Caf4p, Fis1p homologues have been identified in higher eukaryotes, including humans (James et al., 2003).

In *S. cerevisiae*, the number of mitochondria-associated Dnm1p assemblies largely exceeds the number of actual fission events. Many of these assemblies are dynamic and are not localized to tubule constrictions (Legesse-Miller et al., 2003; Naylor et al., 2006). The functional role of the assemblies that are not immediately involved in fission is uncertain. They may represent Dnm1p storage pools, marking future fission sites and, hence, may determine the sites of tubule scission. These assemblies also have been suggested to be involved in attaching mitochondria to the cell periphery (Otsuga et al., 1998). Because none of the currently identified interacting partners of Dnm1p are known to interact with other proteins, except with those of the fission machinery, it is unclear how the localization and the size of these assemblies is controlled.

In this study we used quantitative fluorescence microscopy to investigate the influence of Fis1p, Mdv1p, Caf4p and the actin cytoskeleton on the size, distribution and precise localization of mitochondria-associated Dnm1p assemblies. We employed rotavirus-derived GFP-virus-like particles (GFP-VLPs) (Charpilienne et al., 2001) as an internal calibration standard to estimate the number of Dnm1p molecules within individual assemblies. Next to Dnm1p assemblies, which appear to form spiral-like structures around tubule constrictions, we identified a large number of assemblies that are primarily present at one side of the mitochondrial tubules facing the cell cortex. This polarized localization of the Dnm1p clusters depends on Fis1p and Caf4p, but not on Mdv1, and is maintained in the absence of F-actin. We propose an additional new function of Caf4p in attaching Dnm1p complexes to the cell cortex.

Results

The Dnm1p-GFP pool is almost evenly distributed between mitochondria and cytosol in wild-type cells

For this study, we expressed Dnm1p-GFP from its normal chromosomal locus, replacing the endogenous *DNM1* gene. Mitochondria of cells expressing Dnm1p-GFP fuse and divide and have a normal morphology (Legesse-Miller et al., 2003; Sesaki and Jensen, 1999) (our unpublished results). Hence, we assume Dnm1p-GFP to be fully functional and correctly localized. Previous microscopic studies employing Dnm1p-GFP suggested that a majority of the cellular Dnm1p is concentrated in punctate assemblies (Mozdy et al., 2000; Tieu and Nunnari, 2000). However, according to subfractionation experiments, almost the whole cellular Dnm1p pool is found in the cytosol (Cerveny et al., 2001; Cerveny and Jensen, 2003; Otsuga et al., 1998). These seemingly conflicting but not mutually exclusive findings can be explained by (1) a weak interaction of Dnm1p with the mitochondrial surface that is disrupted upon subfractionation, or (2) by a relatively large Dnm1p-GFP pool that is evenly distributed in the cytosol. In the latter case, the cytosolic Dnm1p-GFP has probably been overlooked by conventional microscopic techniques.

We decided to resolve this question by using very sensitive fluorescence microscopy to quantitatively determine the distribution of the Dnm1p-GFP pool within cells. To this end, we implemented single photon counting avalanche photodiodes in a confocal laser scanning microscope, thereby combining the 3D-resolution capabilities of a confocal microscope with very high fluorescence detection sensitivity. Wild-type (wt) yeast cells (n>80) expressing both Dnm1p-GFP and matrix-targeted red fluorescent protein (mtDsRed) were imaged. To process the image data, a custom-made computer algorithm that discriminates between cytosolic and mitochondria-associated Dnm1p-GFP was used (for details of the algorithm see Materials and Methods). We found that, in wt cells on average 52% of the whole Dnm1p-GFP pool was associated with mitochondria (Fig. 1). We conclude that the larger cytosolic Dnm1p-GFP fraction found in subfractionation experiments is due to a weak and possibly dynamic interaction between Dnm1p-GFP and the mitochondrial surface.

Deletions of *FIS1* or *CAF4* have strong effects on Dnm1p recruitment to mitochondria

Next, we investigated the consequences of deletions of *MDV1*, *FIS1* or *CAF4* on the distribution of the Dnm1p-GFP pool. To assure a very solid statistical groundwork, more than 80 cells of each strain were quantitatively analyzed. In *mdv1Δ* cells, approximately 40% of the whole Dnm1p-GFP pool is associated with mitochondria, so there is a small, albeit statistically significant, difference to the Dnm1p distribution in wt cells (Fig. 1). Hence, in agreement with previous reports (Cerveny and Jensen, 2003; Fekkes et al., 2000; Griffin et al., 2005; Mozdy et al., 2000; Tieu and Nunnari, 2000; Tieu et al., 2002), we found that the deletion of *MDV1* impairs the recruitment of Dnm1p slightly. For Fis1p, a role in recruiting Dnm1p to the mitochondrial surface has been shown (Mozdy et al., 2000; Tieu et al., 2002). Consistently, we found that in cells lacking Fis1p, the fraction of mitochondrial Dnm1p-GFP is decreased to approximately 23% (Fig. 1). In *caf4Δ* cells we detected approximately 29% of the cellular Dnm1p-pool on mitochondria. Hence, deletion of *CAF4* has an effect on the recruitment of Dnm1p-GFP to mitochondria, although in *caf4Δ* cells the mitochondrial Dnm1p-GFP pool is not as strongly

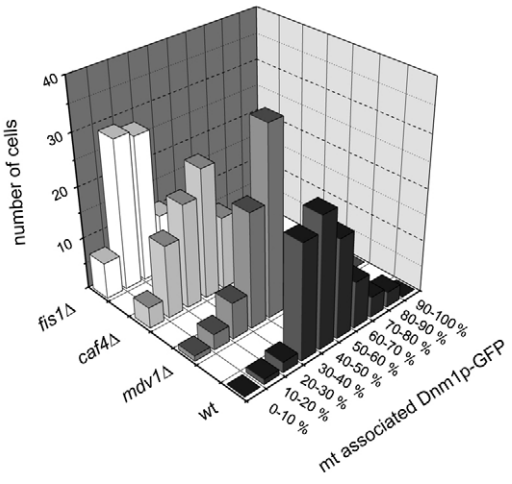

Fig. 1. Deletion of *FIS1*, *CAF4* or *MDV1* influence the relative sizes of the mitochondria-associated Dnm1p-GFP pools. The histogram displays the relative amounts of mitochondria-associated Dnm1p-GFP analyzed on a single-cell basis. 100% equals the whole cellular Dnm1p-GFP pool of the respective cell. For the analysis, fixed cells expressing Dnm1p-GFP and mtDsRed were imaged by using single-molecule-sensitive quantitative confocal fluorescence microscopy. The obtained image data sets were semi-automatically scrutinized. For each strain 80 cells were analyzed.

Table 1. Distribution, number and mean fluorescence intensity of Dnm1p-GFP assemblies

Strain	Mt-associated Dnm1p-GFP assemblies per cell	Mean fluorescence intensity of mt-associated assemblies (normalized)	Cytosolic Dnm1p-GFP assemblies per cell	Mean fluorescence intensity of cytosolic assemblies (normalized)
wt	23.4±0.8	3.5	2.5±0.2	1.3
mdv1Δ	32.3±1.7	4.9	4.8±0.4	1.3
fis1Δ	13.5±0.6	4.1	13.6±0.7	2.2
caf4Δ	28.7±1.2	2.4	17.0±1.7	1.6

The properties of Dnm1p-GFP assemblies in wt, *mdv1Δ*, *fis1Δ*, and *caf4Δ* cells, expressing Dnm1p-GFP and mtDsRed were semi-automatically determined. More than 80 cells were analyzed for each strain. Values are mean ± s.d. The fluorescence intensities were normalized to the mean fluorescence intensity of single GFP-VLPs.

reduced as in *fis1Δ* cells. Mdv1p and Caf4p contribute apparently unequally to Dnm1p recruitment. This observation is in contradiction to a previous study (Griffin et al., 2005), which reported that either Caf4p or Mdv1p is sufficient for efficient recruitment of Dnm1p to mitochondria. The reason for this discrepancy is unclear, but we used a more sensitive fluorescence detection system, which may explain the different results.

We conclude that in wt cells approximately 50% of the Dnm1p pool is assembled on mitochondria. Fis1p and Caf4p are required to maintain this ratio between the cytosolic and the mitochondria-associated Dnm1p pool.

Deletions of *MDV1*, *FIS1* or *CAF4* have different consequences on the number and the size distributions of Dnm1p assemblies

In the following, we investigated the properties of more than 13,000 individual Dnm1p-GFP assemblies, rather than the Dnm1p-GFP pool as a whole (Table 1). In wt cells, on average 23.4±0.8 mitochondria-associated Dnm1p-GFP assemblies were identified, which is in good agreement with previous studies (Cerveny and Jensen, 2003; Tieu et al., 2002). In wt and *mdv1Δ* cells, we found only few cytosolic Dnm1p-GFP assemblies (2.5±0.2 and 4.8±0.4, respectively). The number of cytosolic assemblies is increased in *fis1Δ* and *caf4Δ* cells, which is in agreement with a function of Fis1p and Caf4p in the recruitment of Dnm1p to mitochondria.

To analyze the absolute number of Dnm1p-GFP proteins in individual assemblies, we used the fluorescence intensity of rotavirus-derived GFP-virus-like particles (VLPs) as a scale (Charpilienne et al., 2001; Dundr et al., 2002) (Fig. 2A). Rotavirus is a trilayered virus, which contains the VP2 protein in its innermost layer (Charpilienne et al., 2001; Labbe et al., 1994). When baculovirus assembly is performed in the

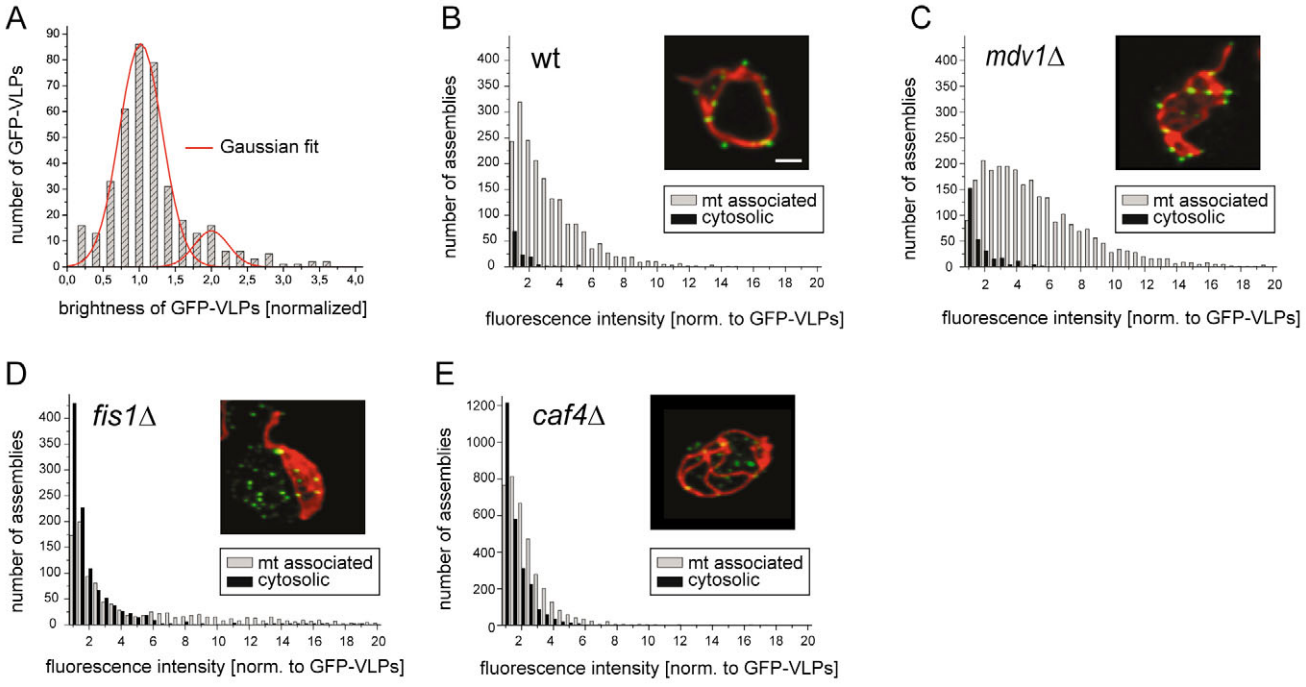

Fig. 2. Cytosolic and mitochondria-associated Dnm1p-GFP assemblies have different size distributions in wt, *mdv1Δ*, *fis1Δ* and *caf4Δ* cells. (A) Fluorescence intensity distribution of GFP-VLPs normalized to 1. The major peak corresponds to single GFP-VLPs, whereas the second peak corresponds to two aggregated GFP-VLPs. A single GFP-VLP contains 120 GFP molecules. (B-E) Fluorescence intensity distributions of mitochondria-associated (gray) and cytosolic (black) Dnm1p-GFP assemblies normalized to the mean fluorescence intensity of single GFP-VLPs. For each graph 80 cells expressing Dnm1p-GFP and mtDsRed were imaged and analyzed. Note the differing *y*-axes values in (E). Insets show representative fluorescence images. Bar, 1 μm.

presence of GFP-tagged VP2 protein, GFP-VLPs containing exactly 120 GFP-VP2 molecules are assembled. The fluorescence intensity of the GFP-VLPs was determined by using the same microscope settings as for imaging Dnm1p-GFP expressing cells. To determine the number of GFP molecules in an individual Dnm1p-GFP assembly the intensity of the assembly was compared with the average intensity value of single GFP-VLPs. The accuracy of this strategy to determine the number of GFP-tagged proteins within tightly packed assemblies has been estimated to be approximately twofold (Dundr et al., 2002). Because a single GFP-VLP exhibits similar fluorescence intensity than most cellular Dnm1p-GFP assemblies, this method is ideally suited to estimate the number of Dnm1p-GFP proteins within an assembly.

We analyzed more than 80 cells from each wt, *fis1Δ*, *mdv1Δ* and *caf4Δ* strains expressing Dnm1p-GFP, and determined the relative fluorescence intensity of more than 13,000 Dnm1p-GFP assemblies. The analysis (for details see Materials and Methods) shows that wt cells contain very few Dnm1p-GFP assemblies with more than 1000 Dnm1p molecules. The deletion of either *FIS1*, *MDV1* or *CAF4* had distinct effects on the sizes of the mitochondria-associated and the cytosolic Dnm1p assemblies (Fig. 2, Table 1). Notably, the number of large assemblies (>1000 molecules per assembly) is increased in *fis1Δ* and *mdv1Δ* cells, whereas in *caf4Δ* cells, similar to wt, very few large assemblies were found.

A majority of Dnm1p-GFP assemblies do not form spirals

Dnm1p belongs to a large family of dynamin-related GTPases that mediate membrane remodelling in a variety of cellular membranes (Hinshaw, 2000; van der Bliek, 1999). The current view on the molecular action of Dnm1p in mitochondrial fission is strongly influenced by our understanding of the role of dynamins (Damke et al., 1995; Hinshaw, 2000; Hinshaw and Schmid, 1995; Sweitzer and Hinshaw, 1998). Dynamins assemble into spirals at the base of clathrin-coated pits to facilitate the scission and release of clathrin-coated vesicles (Takei et al., 1995).

Unconstricted mitochondria have typically a diameter of 350 nm (Egner et al., 2002), which is much larger than the bases of clathrin-coated pits. Several studies found a subset of Dnm1 assemblies at membrane constrictions (Bleazard et al., 1999; Legesse-Miller et al., 2003; Naylor et al., 2006; Sesaki and Jensen, 1999). Moreover, purified Dnm1p forms extended spirals that possess diameters greater than dynamin-1 spirals but that are similar to diameters of mitochondrial constriction sites (Ingerman et al., 2005). Hence, it has been suggested that Dnm1p associates to spirals around mitochondrial constrictions to facilitate fission in vivo. Because of the limited resolution of standard light microscopy (at best approximately 200 nm in the lateral and 500 nm in the axial direction), it is practically impossible to optically resolve a Dnm1p-GFP spiral around a constriction. However, two predictions can be made for a Dnm1p-GFP spiral-like structure at a tubule constriction: (1) The fluorescence signal from the matrix-targeted DsRed is reduced at the constriction site. (2) Since a genuine spiral encircles the constriction evenly, the center of masses of the fluorescence signals from the mtDsRed and the Dnm1p-GFP coincide.

In the following, we denote Dnm1p-GFP structures fulfilling both criteria as Dnm1p-GFP spirals (Fig. 3A-D). We employed a computer algorithm relying on these criteria to identify Dnm1p-spirals in 117 wt yeast cells. All spirals spotted by the algorithm were scrutinized manually. In the end, we found 56 spirals that fulfilled the above criteria in a strict sense. We conclude that at a definite time a vast majority of Dnm1p assemblies do not form unambiguous spirals around tubule constrictions but are located at the side of mitochondrial tubules.

In wt cells most Dnm1p-spirals around a tubule constriction contain 100 to 500 Dnm1 proteins

Although the assembly of Dnm1p spirals appears to be a relatively rare process, it is probably a key event in fission. Thus far, it has been unclear how many Dnm1p molecules form a spiral and whether it is a single ring or a spiral with many turns that is wrapped around a tubule.

To resolve this question, we have estimated the number of Dnm1p-GFP molecules in a spiral by using the fluorescence intensity of single GFP-VLPs as a calibration standard (as described above). In wt cells the spirals displayed a broader distribution of the fluorescence intensities than the GFP-VLPs, demonstrating that the Dnm1p-spirals have varying sizes (Fig. 3E). The fluorescence intensities of the spirals were approximately one to eight times the fluorescence intensity of a single GFP-VLP. The fluorescence intensity of a majority of

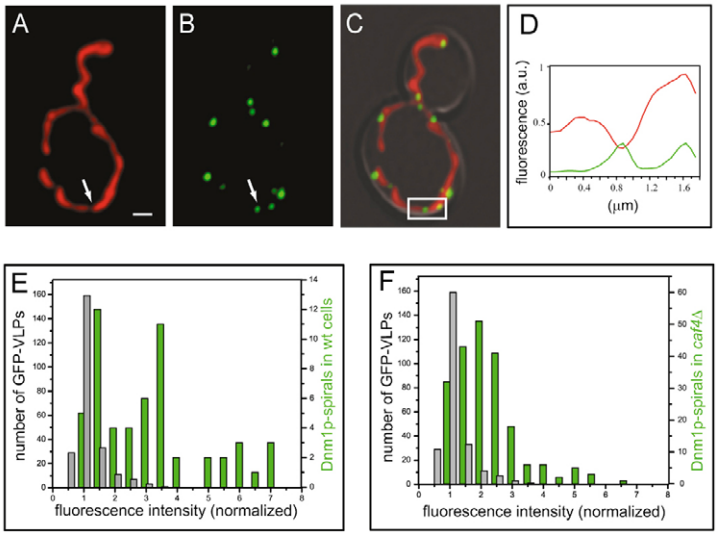

Fig. 3. Tubule constrictions are encircled by a Dnm1p spiral (or rings) that usually contain 100 to 500 Dnm1p molecules. (A-C) Confocal image of a wt cell expressing mtDsRed (A), Dnm1p-GFP (B) and the overlay of both images together with a bright field image (C). The arrow points to a tubule constriction coinciding with a Dnm1p-GFP assembly. Bar 1 μm. (D) Fluorescence intensity profiles in the GFP and DsRed channel (added up in the *y*-direction) within the rectangle shown in C at a tubule constriction. (E,F) Fluorescence intensity distributions of GFP-VLPs (gray) and Dnm1p-GFP spirals (green) normalized to the average fluorescence intensity of a single GFP-VLP in wt (E) and *caf4Δ* cells (F). Note the differing *y*-axes values in E and F. All Dnm1p-GFP spiral-like structures were scrutinized manually. One GFP-VLP contains 120 GFP molecules.

Dnm1p-GFP spirals, however, was one to four times the fluorescence intensity of a single GFP-VLP. Hence, in wt cells most Dnm1p-GFP spirals are formed by 100 to 500 Dnm1p-GFP molecules, which is consistent with a Dnm1p spiral of up to seven turns.

The frequency of Dnm1p-spirals is increased in *caf4Δ* cells

Next, we investigated the frequency of Dnm1p-GFP spirals in *fis1Δ*, *mdv1Δ* and *caf4Δ* cells. Whereas we detected in the wt strain on average 0.4 spirals per cell, this number was reduced close to zero in *fis1Δ* and *mdv1Δ* cells, preventing further analysis. In *caf4Δ* cells the average number of Dnm1p-GFP spirals was increased to approximately two per cell. This difference in the number of Dnm1p-spirals in *mdv1Δ* and *caf4Δ* cells further substantiates the notion that Mdv1p and Caf4p fulfill different cellular roles. Based on the comparatively large number of Dnm1p-GFP spirals in *caf4Δ* cells, we found on average 240 Dnm1p-GFP molecules to form one spiral in this deletion strain, which is in good agreement with the value found in wt cells (Fig. 3F). It will be enlightening to see the reason for the increased number of Dnm1p-GFP spirals in *caf4Δ* cells.

The majority of mitochondria-associated Dnm1p assemblies is spatially oriented towards the cell cortex

Whereas a functional role of Dnm1p spirals is most likely in tubule scission (Ingerman et al., 2005), the function of Dnm1p assemblies that are located at the sides of the tubules is less clear. In the following we will use the term 'cluster' for those mitochondria-associated Dnm1p assemblies that do not form spirals. It has been speculated that Dnm1p has an additional role in attaching the mitochondria to the cell cortex (Otsuga et al., 1998). We reasoned that, in this case, the Dnm1p clusters would be oriented towards the cell wall rather than being randomly distributed on the tubule surface. To test this hypothesis, we investigated the precise localization of Dnm1p-GFP clusters in a large population of cells (>80 cells of each strain) comprising a total of 4500 mitochondria-associated clusters.

We developed a computer algorithm to discriminate between clusters oriented towards the cell cortex, clusters facing the cell interior and those with a sideward orientation (Fig. 4). In live wt cells, the algorithm accounted a small fraction (~20%) of the mitochondria-associated clusters as sideward oriented. These clusters were omitted from further analysis. From the remaining clusters, 78% were oriented towards the cell wall, and only ~22% were facing the cell interior (Fig. 4A). Hence, in live wt cells, most Dnm1p clusters have a polarized orientation and face the cell cortex. Expectedly, this polarized orientation was also observed in chemically fixed cells (Fig. 4A). Because Dnm1p clusters have been described to be highly dynamic (Legesse-Miller et al., 2003), we decided to use in the following fixed cells to investigate the influence of Dnm1p-interacting proteins on the polarity of the clusters.

Fis1p and Caf4p, but not Mdv1p, are required for a polar orientation of Dnm1p-GFP clusters on mitochondrial tubules

The only known interacting proteins of Dnm1p are Fis1p, Caf4p and Mdv1p. In *mdv1Δ* cells, 85% of all analyzable

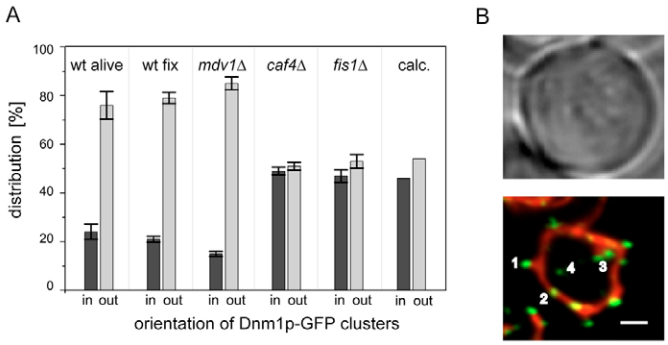

Fig. 4. Fis1p and Caf4p, but not Mdv1p, are required for the polar localization of Dnm1p-GFP clusters on mitochondrial tubules. (A) In wt, *mdv1*Δ, *fis1*Δ, and *caf4*Δ cells expressing Dnm1p-GFP and mtDsRed the precise localizations of mitochondria-associated Dnm1p-GFP clusters were analyzed. The polarity was observed in live and chemically fixed wt cells. The deletion mutants were fixed prior to analysis to avoid spatial movements of the clusters. For each strain more than 80 cells were evaluated. The Dnm1p-GFP clusters point to the cell center (in) or to the cell cortex (out). Due to the curvature of the cell surface, the employed algorithm calculates for randomly distributed mitochondria-associated clusters a slight bias in the distribution (calc.). (B) Top: Bright-field image of a wt cell expressing Dnm1p-GFP and mtDsRed. Bottom: Add-up of confocal sections showing a mitochondrial Dnm1p-GFP cluster pointing to the cell cortex (1), a cluster with a non-analyzable (sideward) localization (2), a mitochondrial Dnm1p-GFP cluster pointing to the cell center (3) and a cytosolic Dnm1p-GFP assembly (4). Only clusters of the categories 1 (out) and 3 (in) were included in the analysis. Bar, 1 μm.

mitochondria-associated clusters were facing the cell cortex, so the polar orientation of the Dnm1p-GFP clusters is independent of Mdv1p (Fig. 4). In cells lacking Fis1p, only 53% of the mitochondria-associated analyzable clusters were on the outside (Fig. 4A). This value is consistent with an entirely random distribution of the Dnm1p-GFP clusters on the mitochondrial surface in *fis1Δ* cells because, due to the curvature of the cell wall, the algorithm calculates for randomly distributed mitochondrial clusters a slight bias of 54% outside and 46% inside (Fig. 4A). Fis1p is evenly distributed on the outer mitochondrial membrane (Mozdy et al., 2000). Thus although required for the polar orientation of Dnm1p clusters, Fis1p seems unlikely to determine the actual directionality of the clusters. However, Fis1p recruits Caf4p to the Dnm1p clusters (Griffin et al., 2005). We find that in cells lacking Caf4p, the mitochondria-associated Dnm1p-GFP clusters are also randomly oriented (Fig. 4), thus pointing to a central role of Caf4p in generating the polarity of the Dnm1p clusters.

Polar localization of mitochondria-associated Dnm1p-GFP clusters is maintained in F-actin-depleted cells

A tempting explanation for the observed polarity is an attachment of the Dnm1p clusters to a cortical structure. In *S. cerevisiae*, a large fraction of the mitochondrial network colocalizes with actin cables (Fig. 5A), suggesting that F-actin interacts, either directly or indirectly, with Dnm1p to determine the polar orientation of the clusters. To investigate this question, wt cells expressing Dnm1p-GFP and matrix-targeted

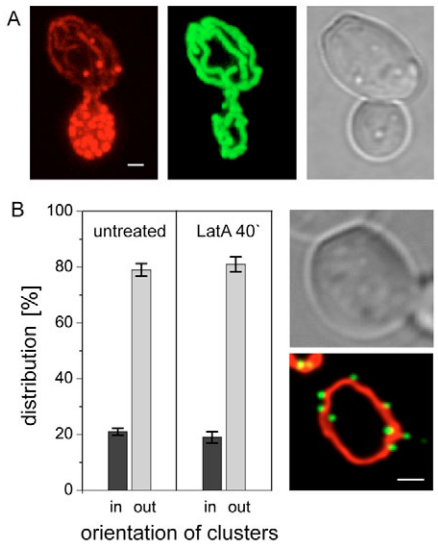

Fig. 5. Polar localization of mitochondrial Dnm1p-GFP clusters is maintained in the absence of F-actin. (A) The actin cytoskeleton partly colocalizes with the mitochondrial network in wt cells. (Left panel) Actin cytoskeleton stained with phalloidin-conjugated Alexa Fluor-546. (Middle panel) GFP-labelled mitochondria. (Right panel) Corresponding bright-field image. (B) Bar graphs show the polarity of the mitochondria-associated Dnm1p-GFP clusters in wt cells treated with the actin depolymerizing drug Latrunculin A for 40 minutes (LatA 40') or without (untreated). A majority of the clusters point to the cell cortex (out). Right: Bright-field and fluorescence image of a representative wt cell treated with Latrunculin A for 40 minutes expressing Dnm1p-GFP and mtDsRed. Bars, 1 μm.

DsRed were treated with the actin depolymerizing drug Latrunculin A. Already after 5 minutes of treatment, actin cables were no longer detectable. Consistent with previous reports (Meeusen and Nunnari, 2003), the mitochondria appeared largely intact even after a 40 min treatment with Latrunculin A. In these cells, 81% of the analyzable clusters still had a polar localization pointing to the cell wall (Fig. 5B). Therefore the polar localization of the Dnm1p clusters is maintained in wt cells for prolonged timed periods in the absence of an intact actin cytoskeleton.

Discussion

In this study, we identified two morphologically distinct subsets of mitochondria-associated Dnm1p assemblies, which probably fulfill different cellular roles. A smaller fraction of the mitochondrial Dnm1p is found at tubule constrictions, apparently encircling the constrictions by spiral-like structures. The majority of the mitochondrial Dnm1p is found in clusters that exhibit a polarized orientation facing the cell cortex. This polarized orientation is abolished in *fis1Δ* and *caf4Δ* yeast, but is maintained in *mdv1Δ* cells. Using sensitive quantitative microscopy, our data corroborate previous findings that the recruitment of Dnm1p to mitochondria is largely abolished in the absence of Fis1p, although a small fraction of Dnm1p still localizes to mitochondria in *fis1Δ* cells (Cerveny and Jensen, 2003; Griffin et al., 2005; Tieu et al., 2002). The deletion of *MDV1* affects Dnm1p recruitment only slightly, whereas the deletion of *CAF4* has a stronger effect on Dnm1p recruitment to mitochondria. Furthermore, in *mdv1Δ* cells the number of apparent Dnm1p-GFP spirals is strongly reduced, whereas it is increased in *caf4Δ* cells. Hence we find that although Mdv1p and Caf4p share a high sequence similarity, their cellular roles appear to be distinct.

Dnm1p associates to spirals of only a few turns around mitochondrial constrictions

Immuno-EM analysis showed that Dnm1p accumulates at sites of mitochondrial constrictions (Bleazard et al., 1999). Based on the decrease of the fluorescence signal of mitochondrial targeted DsRed at constrictions, we estimate the tubule diameter at constrictions to be approximately 100 nm, which is in very good agreement with electron microscopic studies (Ingerman et al., 2005). In vitro, Dnm1p forms extended spirals with a diameter of approximately 110 nm, further supporting that Dnm1p assembles to spiral-like structures at constrictions (Ingerman et al., 2005). Based on the fluorescence intensities of the assembled Dnm1p-GFP, we estimate that most spiral-like Dnm1p structures at tubule constrictions contain 100 to 500 Dnm1p molecules. Dnm1p is highly homologous to dynamin-1, although the diameters of the respective spirals are different (Chen et al., 2004; Ingerman et al., 2005; Zhang and Hinshaw, 2001). If we assume, despite the size differences, a similar molecular architecture of both spirals, approximately 80 Dnm1p molecules make up one helical turn around a 100-nm tubule constriction. Thus we propose that, in vivo, the observed 100 to 500 Dnm1p molecules at a tubule constriction can build a Dnm1p spiral (or rings) with one to a few turns, but generally not a large spiral with more than ten turns. Fission takes probably place at such constrictions encircled by a spiral-like Dnm1p structure (Jensen, 2005; Shaw and Nunnari, 2002).

Our study reveals some variability in the number of Dnm1p molecules assembled at constriction sites. This suggest that Dnm1p-spirals change their architecture during the sequence of the scission process, perhaps reflecting Dnm1p assembly dynamics in fission. Furthermore, at a given point in time, we found in two cells, on average only one unambiguous Dnm1p-spiral, whereas approximately one fission event per minute takes place in a yeast cell (Jakobs et al., 2003a; Nunnari et al., 1997). These observations suggest that Dnm1p spirals are dynamic and short-lived intermediates in the fission process.

A new model for an additional role of Caf4p

Here, we have shown that a subset of Dnm1p assemblies is associated with tubule constrictions, probably forming short spirals with a few turns, whereas the majority of assemblies are primarily present at the side of the tubules. Dnm1p assemblies have been reported to be highly dynamic (Legesse-Miller et al., 2003), so these subsets of assemblies are unlikely to be static over time. The majority of clusters located at the sides of the tubules are directed towards the cell cortex. This polarity depends on Fis1p and Caf4p, but not on Mdv1p. Fis1p is required for efficient recruitment of Caf4p to mitochondria (Griffin et al., 2005). Hence, we assume that Caf4p has a key role in maintaining the polarity of the Dnm1p clusters, and that the loss of Dnm1p-complex polarity in *fis1Δ* cells is a consequence of the impaired Caf4p recruitment in these cells. Mdv1p, by contrast, is apparently not required for Caf4p recruitment, which explains the maintained Dnm1p-cluster

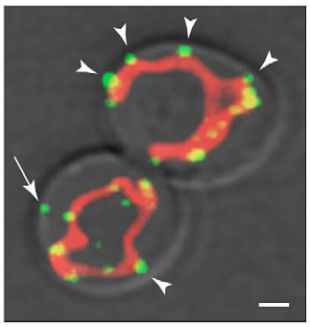

Fig. 6. Polarized mitochondria-associated Dnm1p-GFP clusters appear to be physically attached to the cell cortex. Shown is a wt cell expressing Dnm1p-GFP and mtDsRed after formaldehyde fixation. Displayed is an add-up of confocal sections of the two fluorescence channels overlaid with a bright-field image. After formaldehyde fixation the mitochondrial tubules retract occasionally from the cell cortex, as shown in this image. Arrowheads point to mitochondria-associated Dnm1p-GFP clusters that appear to be attached to the cell cortex. The arrow points to a Dnm1p-GFP cluster that stayed at the cell cortex and might have been torn off from the mitochondrial tubule. Bar, 1 μm.

polarity in *mdv1Δ* cells. The polarity of the clusters might be due to a physical attachment of the clusters to the cell cortex. The model of a cortical attachment of a subset of mitochondrial Dnm1p clusters through Caf4p is supported by two experimental observations.

First, in cells expressing Dnm1p-GFP and matrix-targeted DsRed, it is sometimes observed that upon chemical fixation, the Dnm1p clusters are located at the cell cortex, whereas the mitochondrial tubules retract into the cell interior and appear to hang on the Dnm1p clusters (Fig. 6). This observation suggests a physical connection of the Dnm1p clusters to the cell cortex.

Second, the model that mitochondria are attached to the cell cortex through Dnm1p clusters is in agreement with the previously reported morphologies of the mitochondrial networks in various deletion strains (Griffin et al., 2005): Mitochondria of wt cells have a tubular appearance and are strictly located at the rim of the cell. The mitochondria of *dnm1Δ*, *fis1Δ*, *mdv1Δ/caf4Δ* and *mdv1Δ/dnm1Δ* cells form predominantly nets that are collapsed at one side of the cell (Cerveny et al., 2001; Griffin et al., 2005). The net-like structure of these mitochondria is readily explained by the reduced fission activity (Yaffe, 1999). However, the collapsed net-morphology might be due to a lack of mitochondrial cortex attachment through the Dnm1p/Caf4p complex in each of these strains. By contrast, a large proportion of *mdv1Δ* cells have been reported to exhibit net-like mitochondria that are spread over the cortex rather than being collapsed (Cerveny et al., 2001; Griffin et al., 2005). Again, the net-like structure is due to the reduced fission activity. However, the distribution of the mitochondrial net throughout the rim of the cell might be explained by mitochondrial attachment via a Dnm1p/Caf4p complex to the cell cortex, because Caf4p recruitment is apparently not affected by the deletion of *MDV1*. The similar-to-wt morphology of mitochondria in *caf4Δ* cells is readily explained by assuming that an evenly spread distribution is the energetically most favored form of a tubular network. Previously, the spread-net phenotype in *mdv1Δ* cells has been explained by residual fission activity in *mdv1Δ* cells (Griffin et al., 2005). Both explanations are not mutually exclusive. However, the latter model does not fully explain the similarity of the mitochondrial networks of *dnm1Δ* and *fis1Δ* cells, since cells lacking Fis1p have been reported to display residual mitochondrial fission activity (Jakobs et al., 2003a).

Large parts of the yeast mitochondrial network colocalize with the actin cytoskeleton. In other organisms interactions of Dnm1p/Drp1 with the cytoskeleton have been reported. For example, in HeLa cells, the dynein-dynactin motor protein complex that mediates transport along microtubules, controls recruitment of Drp1 to mitochondria (Varadi et al., 2004). The disruption of the actin cytoskeleton in monkey kidney cells attenuates recruitment of Drp1, suggesting that in these cells actin is involved in the recruitment of Drp1 to mitochondria (De Vos et al., 2005). Our observation that disruption of F-actin does not interfere with the polarized orientation of the Dnm1p clusters on mitochondria, proves that F-actin is not required for the short-term maintenance of cluster polarity in *S. cerevisiae*. Still, the data does not necessarily exclude the possibility that F-actin is involved in recruitment of Dnm1p to the mitochondrial surface in budding yeast, generating the initial polarity of the clusters.

The findings presented in this study indicate the existence of at least two morphologically and possibly functionally distinct sub-sets of mitochondria-associated Dnm1p assemblies, namely spiral-like structures and polarized clusters. Given the spatial and temporal dynamics of the Dnm1p assemblies, it seems likely that these two sub-sets can be converted in each other. It will be enlightening to see further interaction partners of Dnm1p and Caf4p, and to understand the functional implications of the Dnm1p cluster polarity on mitochondrial biogenesis.

Materials and Methods

Yeast-strain constructions

Growth and manipulation of yeast was carried out according to standard procedures (Sherman, 2002). Cells were grown in SC medium with 2% glucose at 30°C to logarithmic growth phase. All strains used in this study were isogenic to BY4741 or BY4742 (Brachmann et al., 1998). The haploid deletion-strains *mdv1Δ*, *fis1Δ* and *caf4Δ* were obtained from Euroscarf (Frankfurt, Germany). Disruptions were confirmed by polymerase chain reaction (PCR).

To generate *DNM1:GFP*, an integrating GFP cassette was PCR amplified with the plasmid pFA6a-GFP(S65T)kanMX6 (Wach et al., 1997) as a template. A spacer of eight amino acids was introduced between Dnm1p and GFP. The following primers were used: The first 36 base pairs of the forward primer are homologous to the 3′ end of *DNM1* (TATAAAAAGGCTGCAACCCTTATTAGTAATATTCTG), omitting the stop codon and followed by 18 bases (GGTCGACGGATCCCCGGG) complementary to the vector sequence. The first 36 base pairs of the reverse primer are homologous to a sequence 95 base pairs downstream of *DNM1* (ATTTTT-ATTAACAAGAAAAAGAATGGAGAGGAGAGCA). The following 18 base pairs of the primer (TCGATGAATTCGAGCTC) anneal to the vector. Integrative epitope-tagging was performed as described (Wach et al., 1997). Deletion strains expressing Dnm1p-GFP were generated by mating of haploid strains, sporulation and tetrad dissection. Genotypes of haploid progeny were determined by PCR.

Plasmid construction

To label the mitochondrial matrix with DsRed, the plasmid pYX222-mtDsRed was constructed. For this vector, the coding sequence of DsRedT4 was amplified by PCR (using the primers GCGGGATCCCCACTAGTCGCCACCATG and CGAAGCTT-CTACAGGAACAGGTGGTG) with pHS12-DsRed.T4 (Bevis and Glick, 2002) as a template. The PCR fragment was digested with *Bam*HI and *Hind*III and inserted into pYX222 (R&D Systems, USA). To target DsRed to the mitochondrial matrix, the subunit 9 (aa 1-69) of the F_0-ATPase of *Neurospora crassa* was excised from pVT100U (Westermann and Neupert, 2000) with *Eco*RI and *Bam*HI and inserted in frame in front of the DsRed sequence.

F-actin disruption

Cells were treated with 250 μM latrunculin A (Molecular Probes, Leiden, Netherlands) for 40 minutes. After washing with PBS, the cells were fixed with 3.7% formaldehyde for 10 minutes. Complete disruption of the actin cytoskeleton was verified by staining with 2.5 μM Alexa Fluor-546 conjugated to phalloidin (Molecular Probes, Leiden, Netherlands) for 1 hour at room temperature.

Microscopy and sample preparation

Cells were harvested by gentle centrifugation (3000 rpm) and fixed in 3.7% formaldehyde for 10 minutes. For imaging, the cells were mounted in 1% low-melting agarose (Sigma, Taufkirchen, Germany) in PBS to inhibit spatial movement of the cells.

A modified beam-scanning microscope (TCS SP2, Leica Microsystems CMS GmbH, Germany) was used for all imaging. Two avalanche photodiodes (Perkin Elmer Optoelectronics, Fremont, CA) attached to the expansion port of the confocal scanning head were used for fluorescence detection instead of the regular photomultiplier tubes.

For image acquisition, a 1.2 numerical aperture water immersion lens (Leica 63×, Planapo) was used. The fluorophores (GFP and DsRed) were simultaneously excited with an Ar-Kr laser line and a HeNe laser at 488 nm and 543 nm, respectively. For all 3D-recordings, the following microscope settings were used: Detection bandpass filters HQ 605/75M and HQ 515/30M (Chroma Technology, Rockingham VT). Detection beam splitter at 560 nm. Pinhole diameter 1 Airy unit. Excitation beam splitter DD 488/543. Voxel size: 0.058 μm, 0.058 μm, 0.162 μm in x, y, z, respectively. 256×256 pixels per image; 4× frame-accumulation; scan speed 400 Hz. For all quantitative image analysis, raw image data were used. Displayed are add-ups of deconvolved confocal sections.

Data analysis

Dnm1p-GFP-cluster localization

A user-written computer algorithm (programmed in C) was employed to semi-automatically determine the precise localization of Dnm1p-GFP clusters on mtDsRed-labeled mitochondrial tubules. In principle, the algorithm processes confocal 3D-data stacks consisting of a GFP and a DsRed channel. It identifies Dnm1p-GFP clusters and determines their fluorescence intensities and their centers of mass (i.e. their position in space). The Dnm1p-GFP localization data was subsequently related to the position of the mitochondrial tubules. By analyzing whether a Dnm1p-GFP cluster adjacent to a mitochondrial tubule is oriented towards the cell interior, the cell cortex, or is non-analyzable (i.e. generally a sideward orientation), the localization of Dnm1p-GFP clusters on the mitochondrial tubules was determined. Further image processing, involving automatic analysis of fluctuations in the mtDsRed signal along a tubule (corresponding to tubule constrictions), was used to identify potential Dnm1p-GFP spiral-like structures. In the following, a more exhaustive description of the employed algorithm is given.

Data acquisition

Confocal 3D-image stacks were cropped manually in both channels to center a single yeast cell in a small data stack (about 5-6 μm in all directions, with a constant voxel size). This data stack, together with manually determined background values were fed into the computer program. The program smoothes the raw data-sets of both channels with a Gaussian filter of sub-diffraction size to reduce noise effects without blurring the imaged structures. The filter is normalized so that the total signal of the data is preserved. Background values are subtracted and the images are corrected for cross-talk (3% cross-talk from the red into the green channel; green to red cross-talk was negligible). Based on these smoothed and background-corrected 3D-data sets, the algorithm iteratively determines the brightness and the relative localization of Dnm1p-GFP assemblies to generate a comprehensive data-set for the subsequent analysis in the following way:

First, the algorithm determines the brightest voxel in the Dnm1p-GFP channel ($I_{max\ Dnm1}$). Around this brightest voxel, a virtual cuboid (290 nm × 290 nm × 810 nm, corresponding to approximately 1.5-times the microscope resolution) is defined in both channels. The center-of-mass in the Dnm1p-GFP cuboid, as well as the average signals in the cuboids of both channels ($I_{avg\ GFP}$ and $I_{avg\ DsRed}$), are determined and stored. Second, the highest signal of the mtDsRed channel on a spherical shell with radius of 150 nm, centered on the Dnm1p-GFP center-of-mass, is determined ($I_{Sphere\ DsRed\ max}$) (supplementary material, Fig. S1). Third, the intensity values on the opposite side of the spherical shell ($I_{Sphere\ DsRed\ otherside}$) and in its center ($I_{Sphere\ DsRed\ center}$) are measured. Fourth, the mtDsRed channel signal on the shell pointing towards the center of the data stack, i.e. the center of the cell, ($I_{Sphere\ DsRed\ inward}$) and at the opposite side of the shell ($I_{Sphere\ DsRed\ outward}$) are determined.

To remove this analyzed Dnm1p-GFP assembly from the further analysis, the point-spread function of an independently recorded fluorescent bead (100 nm) is normalized to $I_{max\ Dnm1}$ and subtracted from a temporary copy of the corrected data-set at the position of the assembly. Following that, the program searches the second brightest voxel in the remaining data-set and repeats the procedure described above until $I_{max\ Dnm1}$ decreases below a pre-defined value. The data obtained by this iterative analysis (for each assembly: $I_{avg\ GFP}$, $I_{avg\ DsRed}$ $I_{Sphere\ DsRed\ max}$, $I_{Sphere\ DsRed\ otherside}$, $I_{Sphere\ DsRed\ center}$, $I_{Sphere\ DsRed\ inward}$, $I_{Sphere\ DsRed\ outward}$) is further processed by spreadsheet analysis.

Discrimination between cytosolic and mitochondrial-associated Dnm1p-GFP assemblies

To discriminate between cytosolic Dnm1p-GFP assemblies and assemblies present at mitochondrial tubules we analyzed the corresponding $I_{avg\ DsRed}$-values: Assemblies with $I_{avg\ DsRed}$ exceeding an experimentally determined threshold were assigned as mitochondria-associated.

Determination of matrix constrictions

To distinguish between Dnm1p-GFP assemblies localized at the side of a tubule and potential spiral-like structures, the ratio of $I_{Sphere\ DsRed\ max}$: $I_{Sphere\ DsRed\ otherside}$ was analyzed. For ratios larger than five, we assigned the Dnm1p-GFP assemblies to the side of the mitochondrial tubules. To analyze whether an assembly, which is not assigned to the side, is located at a matrix constriction, we compared $I_{Sphere\ DsRed\ center}$ with $I_{Sphere\ DsRed\ otherside}$ (see also supplementary material Fig. S1C). For $I_{Sphere\ DsRed\ otherside} > I_{Sphere\ DsRed\ center}$, the corresponding Dnm1p-assemblies were predicted to be at a matrix constriction. All putative Dnm1p-GFP ring-like structures were scrutinized manually.

Analysis of cluster polarity

To discriminate clusters pointing towards the periphery of the cells from those pointing towards the center, the difference ($I_{Sphere\ DsRed\ inward} - I_{Sphere\ DsRed\ outward}$ − correction value) divided by $I_{Sphere\ DsRed\ center}$ was calculated. The (small) correction value was required to compensate for a slightly bent PSF in our microscopic setup. The accuracy of the correction value was verified by computer simulations as well as by control experiments. As an outcome of these calculations, negative values correspond to clusters pointing towards the cell interior (supplementary material in Fig. S1B, blue), whereas positive values correspond to outward-pointing clusters (supplementary material in Fig. S1B, red). Clusters with values between –0.3 and 0.3 were assigned as non-analyzable. Generally these clusters were located at the side of the tubules (supplementary material in Fig. S1B, yellow).

Microscopic size determination of the mitochondria-associated and the cytosolic Dnm1p-GFP pools

To estimate the sizes of the mitochondria associated and the cytosolic Dnm1p-GFP pools, the measured GFP fluorescence intensity of every voxel was assigned to one of theses pools. This analysis was complicated by the fact that the spatial distribution of the signals in the two pools is different: Most mitochondrial associated Dnm1p-GFP is found in assemblies, resulting in a few bright voxels in the microscopic image; the cytosolic Dnm1p-GFP pool comprises – next to a few Dnm1p-GFP assemblies – mostly homogeneously distributed Dnm1p-GFP, which results in very low voxel-intensity values. However, due to the relatively large cytosolic volume these low-level intensity-values may accumulate to a high overall signal that had to be taken into account.

In detail, to accurately determine the sizes of the respective pools, we employed a computer program to create a mask (‘mask 1’) that comprised all voxels of the mitochondria associated pool. Mask 1 comprises two groups (A and B) of voxels. Group A contains all voxels of the mitochondria (identified by high DsRed-voxel values). Group B includes all voxels corresponding to bright Dnm1p-GFP assemblies associated to the mitochondria (including all voxels approximately in the range of the optical resolution of the microscope to account for blurring of the signal within the resolution limit). These voxels were identified by a GFP signal with a threshold slightly above the typical cytosolic signal and at the same time DsRed signal values indicating the vicinity to a mitochondrial tubule due to blur caused by the optical resolution (threshold 25% of the threshold of group A). The correctness of the assignment of these groups to the mitochondrial pool was verified by visual inspection of a substantial set of masks. ‘Mask 2’ was defined as group B – group A.

To determine the cytosolic Dnm1p-GFP pool, all remaining GFP voxel values were summed up resulting in S'_{cyt}. (The voxel values were corrected for background and cross-talk, so that the voxel values outside the yeast cells were on average zero.) To correct for the omitted cytosolic volume defined by mask 2, S'_{cyt} was extrapolated to the complete cytosolic volume. To this end, the volume of a yeast cell (V_{cell}) was estimated to be a sphere with a diameter of 5 μm. The complete cytosolic signal was then extrapolated by using the following formula:

$$S_{cyt} = S'_{cyt} \times (V_{cell} - V_{mask1} + V_{mask2}) \div (V_{cell} - V_{mask1}),$$

with V_{mask1} and V_{mask2} denoting the volumes of the masks.

To obtain the signal S_{mito} of mitochondrial-bound Dnm1p-GFP, S_{cyt} is subtracted from the total GFP signal of all voxels (S_{total}). The relative fractions of Dnm1p-GFP in the cytosol and associated to the mitochondria are obtained by dividing S_{cyt} and S_{mito}, respectively, by S_{total}. For the extrapolation we assumed a homogeneous distribution of Dnm1p-GFP in the cell. Error estimations based on the disregard of the nucleus and the vacuole pointed to a possible error of the order of only 1%, if spherical diameters of 2 μm for both compartments are assumed.

Estimation of the number of Dnm1p-GFP molecules per Dnm1p-GFP assembly

The fluorescence intensity of GFP-virus-like particles (GFP-VLPs) that contain 120 GFP molecules each (Charpilienne et al., 2001) was used as a scale to deduce the number of Dnm1p-GFP molecules in single assemblies. The GFP-VLPs were generously provided by Jean Cohen, CNRS-INRA, Gif-sur-Yvette, France. To ensure that Dnm1p-GFP assemblies and the GFP-VLPs were treated identically for imaging, the GFP-VLPs were fixed in 3.7% formaldehyde for 10 minutes. For imaging, GFP-VLPs were mounted in 1% low-melting agarose (Sigma, Taufkirchen, Germany) in PBS. Image acquisition and data processing of GFP-VLPs was done as with Dnm1p-GFP-expressing cells (see above). The obtained value $I_{avg\ GFP\text{-}VLP}$ was used to calibrate $I_{avg\ Dnm1p\text{-}GFP}$ (for definition see above) to the number of GFP-molecules. Variations between different GFP-VLP preparations were negligible.

We thank S. W. Hell for continuous support and stimulating discussions. We thank J. Cohen for generously providing the GFP-VLPs. We also thank B. Glick (University of Chicago, IL) and B. Westermann (University of Bayreuth, Germany) for providing the plasmids pHS12-DsRed.T4 and pVT100U, respectively. We acknowledge Jaydev Jethwa for carefully reading the manuscript.

References

Bereiter-Hahn, J. and Voth, M. (1994). Dynamics of mitochondria in living cells: shape changes, dislocations, fusion, and fission of mitochondria. *Microsc. Res. Tech*. **27**, 198-219.

Bevis, B. J. and Glick, B. S. (2002). Rapidly maturing variants of the Discosoma red fluorescent protein (DsRed). *Nat. Biotechnol*. **20**, 83-87.

Bleazard, W., McCaffery, J. M., King, E. J., Bale, S., Mozdy, A., Tieu, Q., Nunnari, J. and Shaw, J. M. (1999). The dynamin-related GTPase Dnm1 regulates mitochondrial fission in yeast. *Nat. Cell Biol*. **1**, 298-304.

Brachmann, C. B., Davies, A., Cost, G. J., Caputo, E., Li, J. C., Hieter, P. and Boeke, J. D. (1998). Designer deletion strains derived from Saccharomyces cerevisiae S288c–a useful set of strains and plasmids for PCR-mediated gene disruption and other applications. *Yeast* **14**, 115-132.

Cerveny, K. L. and Jensen, R. E. (2003). The WD-repeats of Net2p interact with Dnm1p and Fis1p to regulate division of mitochondria. *Mol. Biol. Cell* **14**, 4126-4139.

Cerveny, K. L., McCaffery, J. M. and Jensen, R. E. (2001). Division of mitochondria requires a novel Dnm1-interacting protein, Net2p. *Mol. Biol. Cell* **12**, 309-321.

Charpilienne, A., Nejmeddine, M., Berois, M., Parez, N., Neumann, E., Hewat, E., Trugnan, G. and Cohen, J. (2001). Individual rotavirus-like particles containing 120 molecules of fluorescent protein are visible in living cells. *J. Biol. Chem.* **276**, 29361-29367.

Chen, Y. J., Zhang, P., Egelman, E. H. and Hinshaw, J. E. (2004). The stalk region of dynamin drives the constriction of dynamin tubes. *Nat. Struct. Mol. Biol*. **11**, 574-575.

Damke, H., Baba, T., van der Bliek, A. M. and Schmid, S. L. (1995). Clathrin-independent pinocytosis is induced in cells overexpressing a temperature-sensitive mutant of dynamin. *J. Cell Biol.* **131**, 69-80.

De Vos, K. J., Allan, V. J., Grierson, A. J. and Sheetz, M. P. (2005). Mitochondrial function and actin regulate dynamin-related protein 1-dependent mitochondrial fission. *Curr. Biol*. **15**, 678-683.

Dundr, M., McNally, J. G., Cohen, J. and Misteli, T. (2002). Quantitation of GFP-fusion proteins in single living cells. *J. Struct. Biol.* **140**, 92-99.

Egner, A., Jakobs, S. and Hell, S. W. (2002). Fast 100-nm resolution three-dimensional microscope reveals structural plasticity of mitochondria in live yeast. *Proc. Natl. Acad. Sci. USA* **99**, 3370-3375.

Fannjiang, Y., Cheng, W. C., Lee, S. J., Qi, B., Pevsner, J., McCaffery, J. M., Hill, R. B., Basanez, G. and Hardwick, J. M. (2004). Mitochondrial fission proteins regulate programmed cell death in yeast. *Genes Dev*. **18**, 2785-2797.

Fekkes, P., Shepard, K. A. and Yaffe, M. P. (2000). Gag3p, an outer membrane protein required for fission of mitochondrial tubules. *J. Cell Biol.* **151**, 333-340.

Frank, S., Gaume, B., Bergmann-Leitner, E. S., Leitner, W. W., Robert, E. G., Catez, F., Smith, C. L. and Youle, R. J. (2001). The role of dynamin-related protein 1, a mediator of mitochondrial fission, in apoptosis. *Dev. Cell* **1**, 515-525.

Griffin, E. E., Graumann, J. and Chan, D. C. (2005). The WD40 protein Caf4p is a component of the mitochondrial fission machinery and recruits Dnm1p to mitochondria. *J. Cell Biol*. **170**, 237-248.

Hinshaw, J. E. (2000). Dynamin and its role in membrane fission. *Annu. Rev. Cell Dev. Biol*. **16**, 483-519.

Hinshaw, J. E. and Schmid, S. L. (1995). Dynamin self-assembles into rings suggesting a mechanism for coated vesicle budding. *Nature* **374**, 190-192.

Ingerman, E., Perkins, E. M., Marino, M., Mears, J. A., McCaffery, J. M., Hinshaw, J. E. and Nunnari, J. (2005). Dnm1 forms spirals that are structurally tailored to fit mitochondria. *J. Cell Biol.* **170**, 1021-1027.

Jagasia, R., Grote, P., Westermann, B. and Conradt, B. (2005). DRP-1-mediated mitochondrial fragmentation during EGL-1-induced cell death in C. elegans. *Nature* **433**, 754-760.

Jakobs, S., Martini, N., Schauss, A. C., Egner, A., Westermann, B. and Hell, S. W. (2003a). Spatial and temporal dynamics of budding yeast mitochondria lacking the division component Fis1p. *J. Cell Sci*. **116**, 2005-2014.

Jakobs, S., Schauss, A. C. and Hell, S. W. (2003b). Photoconversion of matrix targeted GFP enables analysis of continuity and intermixing of the mitochondrial lumen. *FEBS Lett*. **554**, 194-200.

James, D. I., Parone, P. A., Mattenberger, Y. and Martinou, J. C. (2003). hFis1, a novel component of the mammalian mitochondrial fission machinery. *J. Biol. Chem*. **278**, 36373-36379.

Jensen, R. E. (2005). Control of mitochondrial shape. *Curr. Opin. Cell Biol.* **17**, 384-388.

Labbe, M., Baudoux, P., Charpilienne, A., Poncet, D. and Cohen, J. (1994). Identification of the nucleic acid binding domain of the rotavirus VP2 protein. *J. Gen. Virol.* **75**, 3423-3430.

Legesse-Miller, A., Massol, R. H. and Kirchhausen, T. (2003). Constriction and Dnm1p recruitment are distinct processes in mitochondrial fission. *Mol. Biol. Cell* **14**, 1953-1963.

Meeusen, S. and Nunnari, J. (2003). Evidence for a two membrane-spanning autonomous mitochondrial DNA replisome. *J. Cell Biol.* **163**, 503-510.

Mozdy, A. D., McCaffery, J. M. and Shaw, J. M. (2000). Dnm1p GTPase-mediated mitochondrial fission is a multi-step process requiring the novel integral membrane component Fis1p. *J. Cell Biol*. **151**, 367-379.

Naylor, K., Ingerman, E., Okreglak, V., Marino, M., Hinshaw, J. E. and Nunnari, J. (2006). Mdv1 interacts with assembled Dnm1 to promote mitochondrial division. *J. Biol. Chem*. **281**, 2177-2183.

Nunnari, J., Marshall, W. F., Straight, A., Murray, A., Sedat, J. W. and Walter, P. (1997). Mitochondrial transmission during mating in Saccharomyces cerevisiae is determined by mitochondrial fusion and fission and the intramitochondrial segregation of mitochondrial DNA. *Mol. Biol. Cell* **8**, 1233-1242.

Okamoto, K. and Shaw, J. M. (2005). Mitochondrial morphology and dynamics in yeast and multicellular eukaryotes. *Annu. Rev. Genet.* **39**, 503-536.

Otsuga, D., Keegan, B. R., Brisch, E., Thatcher, J. W., Hermann, G. J., Bleazard, W. and Shaw, J. M. (1998). The dynamin-related GTPase, Dnm1p, controls mitochondrial morphology in yeast. *J. Cell Biol.* **143**, 333-349.

Scott, S. V., Cassidy-Stone, A., Meeusen, S. L. and Nunnari, J. (2003). Staying in aerobic shape: How the structural integrity of mitochondria and mitochondrial DNA is maintained. *Curr. Opin. Cell Biol*. **15**, 482-488.

Sesaki, H. and Jensen, R. E. (1999). Division versus fusion: Dnm1p and Fzo1p antagonistically regulate mitochondrial shape. *J. Cell Biol.* **147**, 699-706.

Shaw, J. M. and Nunnari, J. (2002). Mitochondrial dynamics and division in budding yeast. *Trends Cell Biol*. **12**, 178-184.

Sherman, F. (2002). Getting started with yeast. *Methods Enzymol*. **350**, 3-41.

Smirnova, E., Shurland, D. L., Ryazantsev, S. N. and van der Bliek, A. M. (1998). A human dynamin-related protein controls the distribution of mitochondria. *J. Cell Biol*. **143**, 351-358.

Sweitzer, S. M. and Hinshaw, J. E. (1998). Dynamin undergoes a GTP-dependent conformational change causing vesiculation. *Cell* **93**, 1021-1029.

Takei, K., McPherson, P. S., Schmid, S. L. and De Camilli, P. (1995). Tubular membrane invaginations coated by dynamin rings are induced by GTP-gamma S in nerve terminals. *Nature* **374**, 186-190.

Tieu, Q. and Nunnari, J. (2000). Mdv1p is a WD repeat protein that interacts with the dynamin-related GTPase, Dnm1p, to trigger mitochondrial division. *J. Cell Biol*. **151**, 353-365.

Tieu, Q., Okreglak, V., Naylor, K. and Nunnari, J. (2002). The WD repeat protein, Mdv1p, functions as a molecular adaptor by interacting with Dnm1p and Fis1p during mitochondrial fission. *J. Cell Biol*. **158**, 445-452.

van der Bliek, A. M. (1999). Functional diversity in the dynamin family. *Trends Cell Biol*. **9**, 96-102.

Varadi, A., Johnson-Cadwell, L. I., Cirulli, V., Yoon, Y., Allan, V. J. and Rutter, G. A. (2004). Cytoplasmic dynein regulates the subcellular distribution of mitochondria by controlling the recruitment of the fission factor dynamin-related protein-1. *J. Cell Sci*. **117**, 4389-4400.

Wach, A., Brachat, A., Albertisegui, C., Rebischung, C. and Philippsen, P. (1997). Heterologous His3 Marker and GFP reporter modules for PCR-targeting in Saccharomyces cerevisiae. *Yeast* **13**, 1065-1075.

Westermann, B. and Neupert, W. (2000). Mitochondria-targeted green fluorescent proteins: convenient tools for the study of organelle biogenesis in Saccharomyces cerevisiae. *Yeast* **16**, 1421-1427.

Yaffe, M. P. (1999). The machinery of mitochondrial inheritance and behavior. *Science* **283**, 1493-1497.

Youle, R. J. and Karbowski, M. (2005). Mitochondrial fission in apoptosis. *Nat. Rev. Mol. Cell Biol*. **6**, 657-663.

Zhang, P. and Hinshaw, J. E. (2001). Three-dimensional reconstruction of dynamin in the constricted state. *Nat. Cell Biol*. **3**, 922-926.